Elastic Scattering of 344.5 Mev ^{12}C Ions From ^{11}B Nucleus

S. A. E. KHALLAF
Department of Physics, Faculty of Science,
Assiut University, Assiut - EGYPT
M. A. ABDEL-RAHMAN, S. K. ABDEL-RAHEEM
S. W. Z. MAHMOUD
Department of Physics, Faculty of Science,
El-Minia University, El-Minia - EGYPT

Abstract

The angular distribution of the elastic scattering differential cross section of 344.5 MeV ^{12}C ions from ^{11}B nucleus is calculated and compared with the experimental data as well as the previously published calculations. The real part of the central optical potential is derived using the double-folding and single-folding procedures assuming Gaussian forms of the nucleon-nucleon and alpha-nucleon interactions, respectively. A nuclear matter density distribution function of ^{11}B consisting of a spherical part plus a quadrupole term is used. The inclusion of the quadrupole term is found necessary to obtain good fits to the experimental data.

1. Introduction

Recently, the elastic scattering of ^{12}C on ^{11}B at $E_{lab.} = 344.5$ MeV has been measured [1] between $\theta_{c.m.} = 6.3° - 23.3°$. These data were analyzed using two versions of the optical model: (1) A potential with a Woods-Saxon (WS) form for both the real and imaginary parts, (2) A double folded (DF) potential for the real part of the potential based on the density and energy dependent DDM3Y interaction supplemented by an imaginary potential of WS form. The DF potential required a renormalization factor $N_r = 0.96$ to fit the measured data.

On the other hand, Cook et al [2] have analyzed $^7Li + $ ^{11}B elastic scattering at $E_{lab.} = 34$ MeV in the angular range $10° \leq \theta_{c.m.} \leq 170°$ using DF potential with densities

of the target and projectile consisting of spherical and quadrupole parts. They found that the quadrupole contributions were required to fit the experimental data at large angles.

In the present work, the elastic scattering of $^{12}C +^{11}B$ differential cross section at $E_{\text{lab.}} = 344.5$ MeV is analyzed using the nuclear optical potential, with its real part derived from the double folding (DF) and single folding cluster (SFC) models. The nucleon-nucleon (NN) and the alpha-nucleon (αN) interactions in Gaussian forms are used to calculate the folded potentials through the DF and SFC models, respectively. Also, the nuclear matter distribution of ^{11}B nucleus of Cook et al [2] and a spherical density of ^{12}C nucleus are used. Since we have not the computation facilities of the coupled-channel analysis, the separation vector $\bar{R}$ between the centers of the colliding nuclei is considered parallel to the Z-axis. Accordingly, analytical formulas for the real part of the optical potential dependent on the quadrupole part of ^{11}B density are obtained. These derived potentials supplemented by the imaginary potential of WS form are used to calculate the elastic scattering differential cross sections, which are compared with the experimental data as well as the published phenomenological calculations [1].

2. The Folding Potentials

The double-folding model potential (DF)

The real part of the optical potential is calculated from a more fundamental basis by the folding method in which the NN interaction $V_{NN}(r)$, is folded into the densities of both the projectile and target nuclei [3],

$$V^{DF}(R) = N_r \int \rho_t(r_2)\rho_p(r_1)V_{N-N}(|\bar{R} + \bar{r}_2 - \bar{r}_1|)d\bar{r}_1 \, d\bar{r}_2 \tag{1}$$

where N_r is a free renormalization factor, $\rho_p(r_1)$ and $\rho_t(r_2)$ are the nuclear matter density distributions of both the projectile and target nuclei, respectively, and $V_{NN}(|\bar{R}+\bar{r}_2-\bar{r}_1|)$ is the NN potential.

The effective NN potential considered here has the Gaussian form [4, 5];

$$V_{NN}(r) = \sum_{i=1}^{2} V_i \exp(-K_i \, r^2) \tag{2}$$

where the parameters V_i and K_i are listed in Table (1).

The nuclear matter density distribution of ^{12}C nucleus given by Ref. [6] is;

$$\rho_p(r) = \rho_{oc}(1 + \alpha \, r^2)e^{-\beta \, r^2} \tag{3}$$

with $\alpha = 0.4987 fm^{-2}$, $\beta = 0.37408 fm^{-2}$ and ρ_{oc} can be evaluated from the normalization condition;

$$\int \rho_p(r) \, d\bar{r} = 12 \tag{4}$$

The nuclear matter density distribution of ^{11}B nucleus given by Ref. [2] is;

$$\rho_t(r) = (A + B\, r^2)\, e^{-\gamma^2 r^2} + C\, r^2\, Y_{20}(\hat{r}) e^{-\gamma^2\, r^2} \tag{5}$$

with $A = 0.1943\, fm^{-3}$, $B = 0.09479\, fm^{-5}$, $C = 0.398\, fm^{-5}$, $\gamma^2 = 0.697\, fm^{-2}$ and $Y_{20}(\hat{r})$ is the spherical harmonic of order 2. Substituting Eqns. (2), (3) and (5) into Eqn. (1) and performing a volume integration over $\bar{r}_1$ and $\bar{r}_2$ with $\bar{R}$ parallel to Z-direction one obtains the DF potential $V^{DF}(R)$.

The Single-Folding Cluster Model Potential (SFC)

According to the signle-folding model, the alpha-nucleus potential is calculated by folding an effective αN interaction into the target density [7];

$$V_\alpha^{SF}(R) = N_r \int \rho_t(r)\, V_{\alpha N}(|\bar{R} - \bar{r}|)\, d\bar{r}. \tag{6}$$

In this integral, $V_{\alpha N}$ is chosen in the Gaussian form [6];

$$V_{\alpha N}(r) = V_0\, e^{-k\, r^2} \tag{7}$$

with $V_0 = -37$ MeV and $K = 0.25\, fm^{-2} \cdot \rho_t(r)$ is the nuclear matter density of the target nucleus given by Eqn. (5).

Substituting Eqns. (5) and (7) into Eqn. (6), performing the volume integration over $\bar{r}$ and considering $\bar{R}$ parallel to Z-direction, $V_\alpha^{SF}(R)$ is obtained.

According to the three-alpha cluster model of ^{12}C nucleus, the real part of the central optical potential of ^{12}C-projectile can be expressed as the sum of the three-alpha particle potentials averaged over the internal wave function of ^{12}C nucleus as follows [7]:

$$V^{SFC}(R) = 3 \int |\psi(r,\rho)|^2\, V_\alpha(|\bar{R} + \frac{2}{3}\bar{\rho}|) d\bar{r}\, d\bar{\rho} \tag{8}$$

where $\psi(r,\rho)$ is the relative wave function of ^{12}C nucleus and is given by [8]:

$$\psi(r,\rho) = \left[\frac{2\, (3)^{1/2}\mu}{\pi} \right]^{\frac{3}{2}} \exp\left(-\mu\left(2\rho^2 + \frac{3}{2}r^2 \right) \right) \tag{9}$$

with $\mu = 0.02967\, fm^{-2}$ [9], $\mu = 0.04667\, fm^{-2}$ [10] or $\mu = 0.0884\, fm^{-2}$ [8].

Substituting Eqns. (6) and (9) into (8) and performing the volume integration over $\bar{r}$ and $\bar{\rho}$ one obtains the single folding cluster potential $V^{SFC}(R)$.

Numerical Results and Discussion

The optical model analysis of the experimental data of $^{12}C + ^{11}B$ elastic scattering differential cross section at $E_{\text{lab}} = 344.5$ MeV was calculated using DWUCK4 program [11] feed with either WS forms [1] for both the real and imaginary parts of the nuclear optical potential, or by the DF or SFC real potentials obtained by expressions (1) with (2, 3 and 5) or (8) with (6 and 9), respectively plus a WS imaginary potential of parameters fixed to those shown in Table (3) caption. The Coulomb potential used is that due to a uniform spherical charge distribution of radius $R_c = 1.25(A_p^{1/3} + A_t^{1/3})fm$ [12] where A_p and A_t are the mass number of the projectile and target nuclei, respectively. The renormalization factor, N_r was varied with a step of 0.01 to minimize the quantity

$$\chi^2 = \frac{1}{N} \sum_{i=1}^{N} \left[\frac{\sigma_{th}(\theta_i) - \sigma_{\exp.}(\theta_i)}{\Delta\sigma_{\exp.}(\theta_i)} \right]^2 \tag{10}$$

where N is the total number of the experimental points, $\sigma_{th}(\theta_i)$ is the predicted differential cross section at angle θ_i and $\sigma_{\exp.}(\theta_i)$ and $\Delta\sigma_{\exp}(\theta_i)$ are the experimental cross section and its associated error, respectively, where relative errors of 10 % [1] were taken for computing χ^2.

The data were first fitted with the spherical plus the quadruple $(S. + Q.)$ parts of the DF real potential using the parameters of set A and set B (see Table 1) of NN interaction given by Eqn. (2), separately. The calculated cross sections shown in Fig. (1) fits the available experimental data [1] well over all available angles, but there are deeper minima in case of set A of NN interaction at the scattering angles $\theta_{c.m.} \simeq 10°$ and $15°$. The values of N_r corresponding to the best fit are given in Table (3) for each set of parameters of NN interaction. Set B gives $\chi^2 = 4.83$ while set A gives $\chi^2 = 7.81$. The use of set B gives N_r nearer to unity and smaller χ^2 quantity.

Table 1. Parameters of NN interaction defined by Eqn.(2).

	V_1 MeV	K_1 (fm^{-2})	V_2 (MeV)	K_2 (fm^{-2})	Ref.
Set A	-22.332	0.46	0	0	[4]
Set B	-5.447	0.292	-12.448	0.415	[5]

When the quadruple part of the DF potential is excluded by setting $C = 0$ in Eqn. (5) i.e. spherical potential only $(S.$ only), keeping the same values of N_r, our calculations fitted the differential cross section at forward angles $(\theta < 10°)$ data, but have smaller magnitude and deeper minima at larger angles for the two sets of NN interaction A and B. The optimum potential parameters are shown in Table 3. When the quadrupole contribution is included in the calculations, the deep minima die away at all angles. This seems to be a characteristic feature of the quadrupole coupling [2].

Figure 2 shows the calculated differential cross sections for the system under consideration using SFC potential (dashed curves). The available experimental data are

fitted well over all the angles, but there are deep minima around $\theta_{c.m.} \simeq 10°$ and $15°$, when $\mu = 0.0884$ fm^{-2}. The values of N_r corresponding to the best fit for each value of the parameter μ is obtained and is shown in Table 4.

Table 2. Best fit optical potential parameters (WS) for $^{12}C + ^{11}B$ at 344.5 MeV. The potential has the form given in Ref.[1].

V_0 MeV	r_0 fm	a_0 fm	W_0 MeV	r_W fm	a_W fm	σ_A mb	Ref.
175	0.676	0.9	25	1.13	0.593	1277	[1]

Table 3. Double-folded real optical potential parameters. The imaginary part is of Woods-Saxon form with parameters $W_0 = 20.9$ MeV, $r_W = 1.13$ fm and $a_W = 0.654$ fm taken from ref.[1].

Real part		DF Set A	DF Set B	DDM3Y
Nr	Sph.+Q.	1.3	1.11	
				0.96
	Sph. only	1.3	1.11	
σ_A(mb)	Sph.+Q	1280	1280	
				1287
	Sph.only	1260	1260	
Ref.		Present Work	Present Work	[1]

Table 4. Single-folded cluster real optical poential parameters. The imaginary part is the same as given in Table 3 caption.

μ (fm^{-2})		0.02967	0.04667	0.0884
Nr	Sph.+Q.	1.02	1.17	1.43
	Sph. only	1.02	1.17	1.43
σ_A(mb)	Sph.+Q	1280	1290	1270
	Sph.only	1260	1260	1260

Exclusion of the quadrupole part of the SFC real potential by setting C=0 in Eqn. (5) results in fitting the differential cross section in the forward angles ($\theta < 10°$) region, but have a smaller magnitude and deeper minima at larger angles in all cases of the parameter μ (dotted curves in Figure 2). The optimum potential parameters are shown in Table 4. It is obvious from these calculations which include the quadrupole contribution (dashed curves) that the deeper minima die away at all angles and the value

of $\mu = 0.02967$ fm^{-2} is the most suitable for the best fit with $\chi^2 = 3.31$, while other values of μ give higher values of χ^2 e.g. 6.37 and 9.62 for $\mu = 0.04667$ fm^{-2} and 0.0884 fm^{-2}, respectively and less satisfactory fits to the data. Moreover, $N_R = 1.02$ and the value of σ_A is very close to that value of WS potential shown in Table 2 in case of μ=0.02967 fm^{-2}.
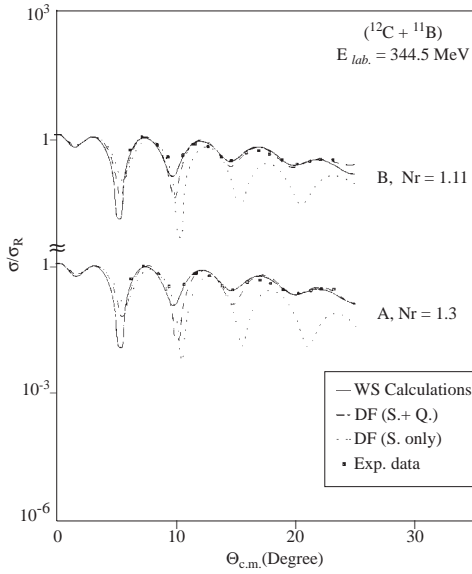
Figure 1. Comparison between the differential cross sections as ratio -to- Rutherford for the elastic scattering of ^{12}C on ^{11}B at 344.5 MeV calculated with DF real central potential using A and B sets of *NN* interaction and the imaginary part of parameters given in Table 3 caption. Solid curves are the WS calculations with parameters of Table 2, dashed-curves are the spherical + quadrupole (S.+Q.) DF calculations, the dotted-curves are the spherical (S.) DF calculations and the solid points are the experimental data taken from Ref.[1].
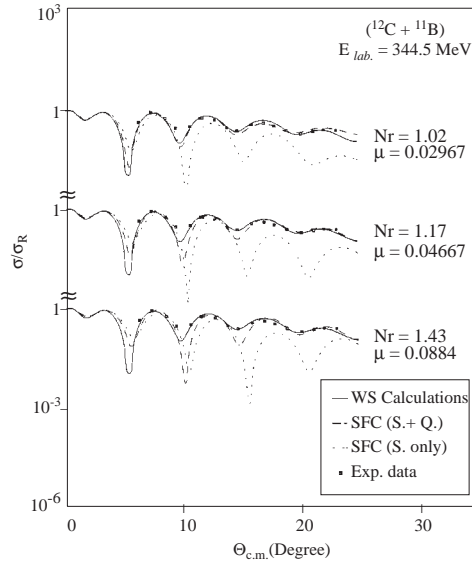
Figure 2. Comparison between the differential cross sections as ratio -to- Rutherford for the elastic scattering of ^{12}C on ^{11}B at 344.5 MeV calculated with SFC real central potential using different values of the parameter μ of the internal wave function of ^{12}C nucleus and the imaginary WS potential of parameters given in Table 3 caption. Solid curves are the WS calculations with parameters of Table 2, dashed-curves are the (S.+ Q.)puadrupole SFC calculation, the dotted-curves are the (S.) SFC calculations and the solid points are the experimental data of Ref.[1]

In Figure 3 the renormalized DF real potentials (S.+Q.) and (S. only) are compared with the real WS potential of parameters given in Table 2, while Figure 4 shows the renormalized SFC real potentials (S.+Q.) and (S.only), for the different values of the parameter μ compared with the same real WS potential. In all cases, the S.+ Q. potential

is closer to the WS potential specially in the region of the strong absorption radius (4-6 fm), but significant differences occur in the tail region, while the corresponding potentials with only spherical part have smaller magnitudes in this region. This may indicate that the calculated elastic scattering differential cross section of the system under investigation is sensitive to the real potential in the vicinity of the strong absorption radius while the tail region of the potential has a less effect on the cross section.

From Tables 3 and 4, it is clear that the absence of the quadrupole term in DF and SFC potentials slightly reduces the reaction cross section, σ_A, while the presence of this term increases the value of σ_A to be in agreement with that obtained from a previous analysis of the system [1]. Also, the value of the parameter $\mu = 0.02967$ fm^{-2} gives σ_A equal to that obtained from the DF model analysis in the present work and nearly the same value of the previous DF model with DDM3Y interaction [1].
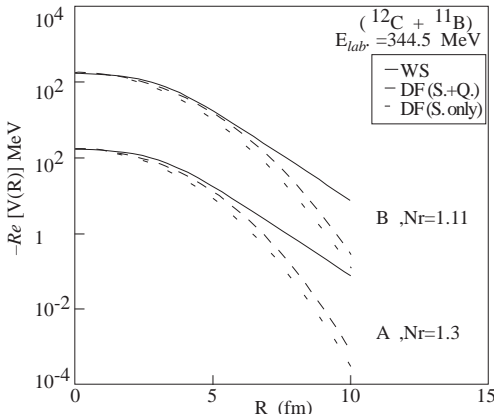
Figure 3. Comparison of the DF and WS real potentials for $^{12}C + ^{11}B$ elastic scattering at 344.5 MeV for the two sets of NN interaction (A,B), solid curves are the real WS potential of parameters given in Table 2, dashed-curves are the renormalized (S.+Q.) DF potential and the dotted-curves are the renormalized (S.) DF potential. The renormalization factors N_r are given in table 3.
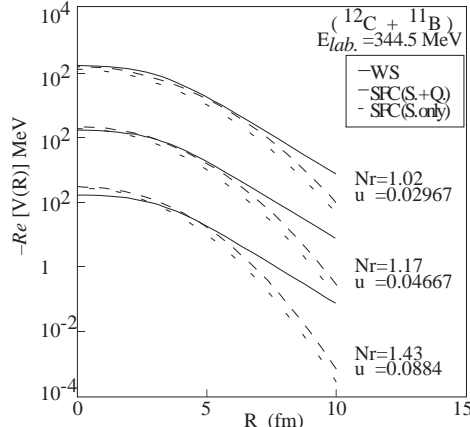
Figure 4. Comparison of the SFC and WS real potentials for $^{12}C + ^{11}B$ elastic scattering at 344.5 MeV for different values of the parameter μ of the internal wave function of ^{12}C nucleus, solid curves are the real WS potential of parameters given in Table 2, dashed-curves are the renormalized (S.+Q.) SFC potential and the dotted-curves are the renormalized (S.) SFC potential. The renormalization factors N_r are given in Table 4.

Finally, it may be concluded that using an integrable Gaussian form of NN interaction in DF method or αN interaction in SFC method described in the present work predicts well the real central part of the optical potential as well as the elastic scattering cross section for the system $^{12}C + ^{11}B$ at $E_{lab.} = 344.5$ MeV. Also, the quadrupole part

of the nuclear matter density distribution of ^{11}B nucleus is more sensitive in the prediction of the real central potential and the elastic scattering cross section even at this small range of angles ($\theta_{c.m.} < 24°$) considered here. It may be useful to mention here that Cook et al [2] and Parks et al [13] found that the quadrupole contributions were required to fit the elastic scattering data of the system $^{7}Li +^{11}B$ at 34 MeV and $^{11}B +^{27}Al$ at 50 MeV, respectively, at larege angles. Use of the coupled-channel procedure and an energy-densitiy dependent NN interaction in the analysis may reduce the renormalization factor, N_r to unity. The density distribution function and the internal wave function are also important.

Acknowledgement

References

[1] L. Jarczyk, B. Kamys, A. Magiera, R. Siudak, A. Strzalkowski, B. Styczen, J. Hebenstreit, W. Oelert, P. Von Rossen, H. Seyfarth and G. R. satchler 1990 *Nucl. Phys.* **A 518** 583; R. Siudak private communication.

[2] J. Cook, M. N. Stephens and K. W. Kemper 1987 *Nucl. Phys.,* **A466** 168.

[3] G. R. Satchler and W. G. Love 1979 *Phys. Rep.* **55** No. 3 183.

[4] W. G. Greenless, G. J. Pyle and Y. C. Tang 1968 *Phys. Rev.* **171** 1115.

[5] J. B. Ball, C. B. Fulmer, E. E. Gross, M. K. Halbert, D. C. Hensley, C. A. Ludemann, M. J. Saltmarsh and G. R. satchler 1975 *Nucl. Phys.* **A252** 208.

[6] H. M. Hussein and O. Zohni 1976 *Nucl. Phys.* **A267** 303.

[7] S. A. E. Khallaf, A. L. Elattar and Farid M. El-Azab 1983 Fizika 125.

[8] M. W. Kermode, 1964 *Proc. Phys. Soc.* **84** 554.

[9] S. A. E. Khallaf, A. L. Elattar and Farid M. El-Azab 1982 *J. Phys.* **G8** 1721.

[10] S. A. E. Khallaf, Farid M. El-Azab 1981 *Atomkernenergie/Kerntechnik* **37** 294.

[11] P. D. Kunz 1969 DWUCK4 program, University of Colorado (unpublished).

[12] S. Albergo, S. Costa, R. Potenza, J. Romanski and C. Tuve 1991 *Phys. Rev. C* **43** 2704.

[13] L. A. Parks, K. W. kemper, A. H. lumpkin, R. I. Cutler, L. H. Harwood, D. Stanley, P. Nagel and F. Petrovich 1977 *Phys. Lett.* **70B** 27.